Loss-of-function BK channel mutation causes impaired mitochondria and progressive cerebellar ataxia

Xiaofei Du[a,1], Joao L. Carvalho-de-Souza[b,c,1,2], Cenfu Wei[a], Willy Carrasquel-Ursulaez[d,3], Yenisleidy Lorenzo[d], Naileth Gonzalez[d], Tomoya Kubota[b,c,4], Julia Staisch[a,5], Timothy Hain[e], Natalie Petrossian[a], Michael Xu[a], Ramon Latorre[d], Francisco Bezanilla[b,c,d], and Christopher M. Gomez[a,6]

[a]Department of Neurology, The University of Chicago, Chicago, IL 60637; [b]Department of Biochemistry and Molecular Biology, The University of Chicago, Chicago, IL 60637; [c]Institute for Biophysical Dynamics, The University of Chicago, Chicago, IL 60637; [d]Centro Interdisciplinario de Neurociencia de Valparaíso, Facultad de Ciencias, Universidad de Valparaiso, Valparaíso 2340000, Chile; and [e]Department of Neurology, Northwestern University, Chicago, IL 60611

Edited by David Julius, University of California, San Francisco, CA, and approved January 30, 2020 (received for review November 22, 2019)

Despite a growing number of ion channel genes implicated in hereditary ataxia, it remains unclear how ion channel mutations lead to loss-of-function or death of cerebellar neurons. Mutations in the gene *KCNMA1*, encoding the α-subunit of the BK channel have emerged as responsible for a variety of neurological phenotypes. We describe a mutation (BK_{G354S}) in *KCNMA1*, in a child with congenital and progressive cerebellar ataxia with cognitive impairment. The mutation in the BK channel selectivity filter dramatically reduced single-channel conductance and ion selectivity. The BK_{G354S} channel trafficked normally to plasma, nuclear, and mitochondrial membranes, but caused reduced neurite outgrowth, cell viability, and mitochondrial content. Small interfering RNA (siRNA) knockdown of endogenous BK channels had similar effects. The BK activator, NS1619, rescued BK_{G354S} cells but not siRNA-treated cells, by selectively blocking the mutant channels. When expressed in cerebellum via adenoassociated virus (AAV) viral transfection in mice, the mutant BK_{G354S} channel, but not the BK_{WT} channel, caused progressive impairment of several gait parameters consistent with cerebellar dysfunction from 40- to 80-d-old mice. Finally, treatment of the patient with chlorzoxazone, a BK/SK channel activator, partially improved motor function, but ataxia continued to progress. These studies indicate that a loss-of-function BK channel mutation causes ataxia and acts by reducing mitochondrial and subsequently cellular viability.

KCNMA1 | ataxia | cerebellar degeneration

Mutations in a wide array of ion channel genes underlie distinct forms of neurological disease. Prominent among these are the spinocerebellar ataxias (SCAs) that are a group of genetically diverse neurodegenerative diseases affecting the cerebellum and its connections. Approximately one-third of the nearly 30 genetically identified forms of autosomal-dominant cerebellar ataxia are due to mutations in ion channel genes, including genes for four distinct voltage-gated potassium channels (K_V) (1–11). Missense mutations of the *KCNA1* (Kv1.1), *KCNC1* (Kv3.1), *KCNC3* (Kv3.3), and *KCND3* (Kv4.3) K^+ channel genes underlie episodic or progressive ataxia syndromes, and some of them are associated with cognitive impairment and/or epilepsy (1, 3–7). The human *KCNMA1* gene encodes the large-conductance, calcium- and voltage-activated K^+ (BK) channel α-subunit. The BK pore-forming α-subunit contains seven transmembrane segments (S0 to S6) with an extracellular N terminus and an extensive intracellular C terminus containing two high-affinity Ca^{2+} binding sites (12). BK channels are activated by both membrane depolarization and cytosolic Ca^{2+}. Mutations in the BK channel lead to a variety of clinical syndromes, correlated in part to the molecular phenotype, roughly divided into gain-of-function (GOF) and loss-of-function (LOF) (13). Du et al. identified a single missense mutation (D434G) in *KCNMA1* that leads to a GOF change in BK channel and causes autosomal-dominant epilepsy with paroxysmal dyskinesias in a large kindred (14). Several individual patients have been reported with a *KCNMA1* variant predicting a point mutation (variably designated as N995S/N999S/N1053S) in the BK channel associated with epilepsy without dyskinesia. Interestingly, whereas the GOF phenotype of the D434G mutant is due to an increase in the BK Ca^{2+} sensitivity, in the N995S mutant the BK GOF is due to a leftward shift of the conductance–voltage (*G–V*) curve. LOF mutations, which reduce either channel current or protein expression, are more consistently associated with cerebellar involvement and intellectual disability (ID), with variable presence of seizures, dyskinesias, and dystonia (13, 15). Moreover, mice lacking the BK channel developed cerebellar ataxia and Purkinje cell dysfunction (15). More recently, several rare *KCNMA1* mutations producing an array of pathological phenotypes were reported (13, 16). However, other than the common theme of disturbed ion channel function, there is as yet little insight as to how the reported *KCNMA1*

Significance

Genetic disruption of ion channels underlies several neurological diseases, suggesting that ionic disturbances are common neuronal stressors potentially amenable to therapies. The detailed intracellular pathways coupling ion channel mutations to neuronal damage are largely unknown. Here, we describe the finding of a single loss-of-function mutation in the BK channel in a young patient with progressive cerebellar degeneration. The mutant BK channel caused a profound dominant-negative effect on native channels, combined with reduced ion selectivity, leading to depolarization and depletion of mitochondria, and when delivered virally to mice, mimicked the disease. BK channel active drugs rescued the mutant cellular phenotype. These results point to the importance of mitochondrial ionic homeostasis in cerebellar disease and suggest therapeutic strategies.

Author contributions: X.D., J.L.C.-d.-S., R.L., F.B., and C.M.G. designed research; X.D., J.L.C.-d.-S., C.W., W.C.-U., Y.L., N.G., T.K., J.S., T.H., N.P., and M.X. performed research; X.D., J.L.C.-d.-S., C.W., T.K., J.S., T.H., R.L., F.B., and C.M.G. analyzed data; and X.D., J.L.C.-d.-S., R.L., F.B., and C.M.G. wrote the paper.

The authors declare no competing interest.

This article is a PNAS Direct Submission.

Data deposition: All DNA plasmids and bacterial strains used in this study are available at Dryad (https://doi.org/10.5061/dryad.1ns1rn8qk).

[1]X.D. and J.L.CdS contributed equally to this work.

[2]Present address: Department of Anesthesiology, University of Arizona, Tucson, AZ 85724.

[3]Present address: Department of Neuroscience, University of Wisconsin–Madison, Madison, WI 53706.

[4]Present address: Department of Biomedical Informatics, Osaka University Graduate School of Medicine, Suita, Osaka 565-0871, Japan.

[5]Present address: Department of Neurology, Ochsner Medical Center, New Orleans, LA 70121.

[6]To whom correspondence may be addressed. Email: cgomez@neurology.bsd.uchicago.edu.

This article contains supporting information online at https://www.pnas.org/lookup/suppl/doi:10.1073/pnas.1920008117/-/DCSupplemental.

First published March 4, 2020.

mutations lead to neurological diseases (17–19). Here, we describe a LOF mutation, identified by exome sequencing, in the *KCNMA1* gene encoding BK channel α-subunit (BK_{G354S}) associated with progressive cerebellar degeneration, ataxia, and cognitive impairment due to cellular toxicity and dysfunction/depletion of mitochondria.

We evaluated a 16-y-old girl who presented with cognitive impairment, multifocal dyskinesias, and progressive ataxia. Using exome sequencing, we identified a de novo mutation in the *KCNMA1* gene predicting the mutation G354S in BK channels. The glycine residue 354 is in the BK selectivity filter, a highly conserved amino acid sequence among K^+-selective ion channels. BK channels composed of the G354S mutant α-subunits (BK_{G354S}) exhibit a dramatically reduced unitary conductance relative to BK channels bearing wild-type (WT) α-subunits (BK_{WT}) and proportional reduction in the macroscopic K^+ currents, suggesting no changes in protein abundance. Importantly, the mutation also reduces BK channel selectivity to K^+ ions, increasing the relative permeability to Na^+ ions. Expression of BK_{G354S} also led to reductions in neurite outgrowth and cellular viability, together with depletion of mitochondria when expressed in cultured neuronal cells. Notably, application of the BK channel activator NS1619 (20–22) activates the WT channels, while inhibiting the mutant BK channels, to improve viability and mitochondrial content in cultured cells. Viral delivery to neonatal mice of the BK_{G354S} channel, but not the BK_{WT} channel, caused impaired gait. Clinically, treatment of the patient with chlorzoxazone, a pharmaceutical SK/BK channel activator (23), slightly improved motor coordination scores and balance, although the ataxia continued to progress. This study describes an association of progressive ataxia with a mutation in the BK channel and supports the view that BK channel function, particularly in mitochondria, is critical for neuronal viability and is a potential mechanism for Purkinje cell degeneration and cerebellar ataxia.

Results

Clinical Phenotype and Identification of the BK Channel G354S Mutation. The patient, a 16-y-old female, was noted to have ataxic gait and delayed motor milestones at the age of 18 mo. Clinical features are summarized in Table 1 and compared with those bearing previously reported *KCNMA1* mutations (14, 17–19, 24). She had two febrile seizures between 3 and 5 y of age. She was developmentally delayed, estimated to read at a first-grade level, and exhibited emotional outbursts. Her language comprehension was slightly subnormal, but she had an unintelligible speech due to severe dysarthria. Her motor coordination initially improved but lagged behind that of her younger sister, until at 8 y of age when she began to have slow deterioration in her gait and upper limb coordination. She developed scoliosis at age 14, but only required conservative management. At the age of 16, her neurological examination revealed slight difficulties with comprehension and following conversations, but good orientation and memory. She also showed coarse downbeat and gaze-evoked nystagmus in all directions; perioral, truncal, and limb dyskinesias; slightly spastic tone with bilateral Babinski signs; frank anarthria, intention tremor, past pointing, and dysdiadokinesia in her limbs; and severely wide-based and unsteady stance and gait. Her biological parents and younger sister are alive and doing well with no neurological complaints. Serial MRI scans from age 7 to 15 revealed severe and progressive cerebellar atrophy, most prominent in the midline, and no other abnormalities of cerebral hemispheres (Fig. 1*A*). The morphometric analysis estimated a 20% loss of cerebellar volume over 8 y.

Whole-exome sequencing (WES), followed by targeted di-deoxy sequencing of proband, parents, and unaffected sister, confirmed four heterozygous de novo variants in the proband (*SI Appendix*, Table S1). The mutation most likely to be associated with the patient's symptoms was a 1060 G>A mutation in exon 8 in the *KCNMA1* gene, which encodes the BK channel, suggesting a G354S amino acid change in this protein (Fig. 1*B*).

This mutation was not present in any database, including the Exome Aggregation Consortium (ExAC) and gnomAD databases of aggregated WES data, or in 765 exomes sequenced at University of Chicago, including 322 other patients with ataxia. The residue G354 is conserved in the sequence of amino acids that forms the selectivity filter of K^+ channels, 352-TVGYG-356. This motif is conserved in BK channels identified at least as far back as *Drosophila* (Fig. 2). In silico genetic prediction algorithms, such as SIFT and PolyPhen-2, that use sequence- and structure-based features and evolutionary conservation of amino acids predicted this substitution to be pathogenic (25, 26).

Of the three other de novo variants identified in WES, a variant in SLC22A5 suggests that the patient is also a possible carrier of carnitine deficiency (27) (*SI Appendix*, Table S2), while the two others DYSF and BRAT1 are associated with recessively inherited syndromes (28, 29) and have been seen in the normal population (https://gnomad.broadinstitute.org/).

BK_{G354S} Channels Have Dramatically Reduced K^+ Conductance, and Lower Selectivity to K^+. The G354S mutation in BK channels is located in the channel selectivity filter, the narrowest part of the conducting pathway (30). Since G354 is one of the residues that coordinate K^+ ions with its carbonyl group during conduction, we hypothesized G354S mutation would cause changes in the unitary conductance as well as in the ionic selectivity to K^+. To study the effects of the G354S mutation on conductive properties of BK channels, we separately expressed BK_{G354S} and BK_{WT} channels in *Xenopus* oocytes. Based on the fact the proband bears both WT and a mutant allele of the *KCNMA1* gene, we also coinjected oocytes with equal amounts of both WT and mutant complementary RNA (cRNA), to explore the possible dominant-negative effect of BK_{G354S} on channels also containing

Table 1. Summary of clinical features in proband compared with subjects with other reported *KCNMA1* mutations

	BK mutations														
	LOF mutations											GOF mutations			
Symptoms	S351Y (16)	G354S	G356R (16)	G375R (16)	N449fs*/C413Y (16)	R458ter* (19)	I663V (16)	Y676Lfs*7 (17)	P805L (16)	G884L (18)	D984N (16)	D434G (14)	N995S (23)	N999S (23)	N1053S (18)
Zygosity	Het	Het	Het	Het	Compound het	Homo	Het	Homo	Het	Het	Het	Het	Het.	Het	Het
Age of onset	Inf	18 mo	Inf	Inf	NA	Inf	Inf	8 mo	Inf	20 d	Inf	2 y	9 y	20 mo	7 mo
Ataxia	+	+	—	—	+	+	+	—	—	—	—	—	—	—	—
Seizure type	—	Febrile	—	Abs	—	GTC/atonic	NA	Myoclonic/GTC2/3	—	—	Gen, focal dystonic	Abs/GTC	GME	Atypical abs myoclonic	—
Dyskinesias/Dystonia	NA	+	++	NA	—	+	+	—	—	++	+	++	—	4/7	—
Nystagmus	—	+	—	+	—	NA	—	—	—	+	—	—	NA	NA	—
DD/ID	+	+	++	++	++	++	+	++	+	++	+	—	—	+	+
Cerebellar atrophy	—	+	+	+	+	+	—	+	—	—	—	—	—	—	—
Developmental anomalies	Facial, digital	+	Skeletal	Facial, visceral	Facial	—	—	NA	—	NA	—	NA	NA	NA	NA

— indicates absent, + indicates present, and ++ indicates moderate to severe. abs, absent; DD/ID, developmental delay/intellectual disability; Gen, generalized; Het, heterozygous, Homo, homozygous; Inf, infancy; NA, not available.

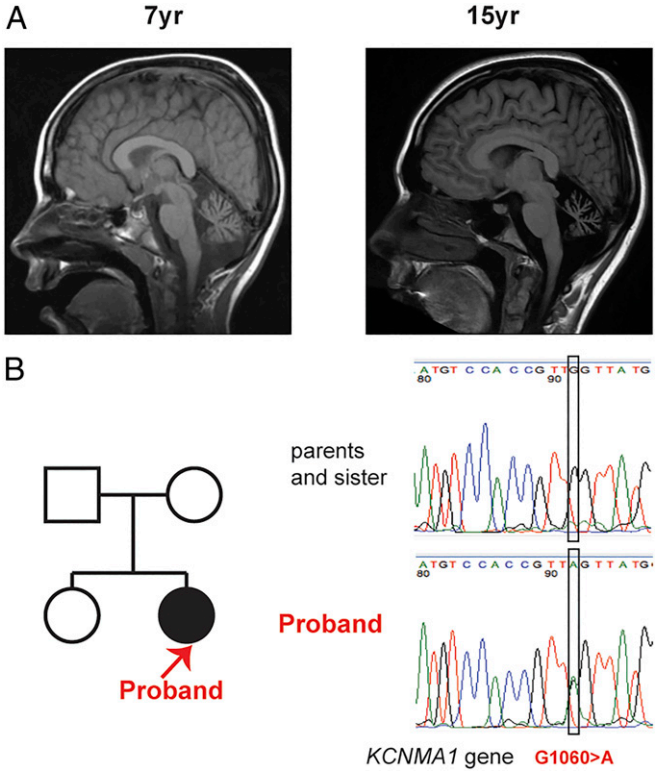

Fig. 1. Serial MRI scans and direct Sanger sequence of the patient with *KCNMA1* gene c.1060G>A mutation. (*A*) Serial MRI scans of the patient from age 7 to 15 y. Midline sagittal T1-weighted images of the patient at 7 y and at 15 y of age demonstrating pronounced selective atrophy of the cerebellum. (*B*) Direct Sanger sequence of *KCNMA1* gene mutation region of the patient, sister, and parents. (*Left*) Pedigree of the family with c.1060G>A AD mutation on the chromosome 10. (*Right Upper*) The direct representative sequence of *KCNMA1* c.1060G region at exon 8. (*Right Lower*) The heterozygous mutation of c.1060G>A (p.G354S) in the patient. The box indicated the location of the mutation.

BK_{WT}: $BK_{WT\text{-}G354S}$. In all three cases (BK_{WT}, $BK_{WT\text{-}G354S}$, and BK_{G354S}), we recorded robust macroscopic K^+ currents consistent with different levels of conductance (*SI Appendix*, Fig. S1*A*). Oocytes injected with 50 ng of cRNA for BK_{G354S} showed on average (n = 10) 11% of the maximal current compared with oocytes injected with only 25 ng of cRNA for BK_{WT}. Considering that oocytes can proportionally express channels according to the amount of cRNA injected, in the range between 25 and 50 ng, we could speculate that oocytes injected with 25 ng would express one-half of the number of channels than those injected with 50 ng. Therefore, the 11% translates to 5.5% when normalized by the amount of cRNA injected. The oocytes injected with both types of cRNA, WT and mutant, 25 ng each, served to probe the dominant-negative effect of BK_{G354S} on heterochannels, the $BK_{WT\text{-}G354S}$. If the oocytes were to express both channels equally but independently, without forming heterochannels, the level of current recorded from these oocytes would be at least the same as in those oocytes expressing BK_{WT} only. Surprisingly, the oocytes injected with 25 ng of each cRNA for BK_{WT} and BK_{G354S} showed 45% of the currents from the BK_{WT} group of oocytes (*SI Appendix*, Fig. S1*B*). We also analyzed the kinetics of the K^+ current activation. The currents from BK_{G354S} were activated up to two orders of magnitude slower than the currents from BK_{WT}. Interestingly, the time constants from $BK_{WT\text{-}G354S}$ were only two to six times slower than the currents from BK_{WT} (*SI Appendix*, Fig. S1*C*). Altogether, these data strongly suggest the BK_{WT} and BK_{G354S} coassemble to form heterochannels and that the BK_{G354S} channels exert a dominant-negative effect on $BK_{WT\text{-}G354S}$ heteromers.

Currents Recorded from BK_{G354S} in Oocyte's Macropatches. Voltage clamping of macropatches of membranes expressing BK_{G354S} also showed reduced currents compared to a comparable experiment with membranes expressing BK_{WT}. Since the activation of BK channels is controlled by voltage as well as by intracellular concentration of Ca^{2+}, very low intracellular Ca^{2+} concentration in cut-open oocyte experiments results in channel activation at very positive voltages (with $V_{1/2}$ around +170 mV), well beyond the efficient range in the cut-open oocyte preparation. Experiments with macropatches are appropriate for a wider range of voltages and have the additional advantage that Ca^{2+} concentration can be controlled both inside and outside the membrane (Fig. 3 *A* and *B*). Channel activation in macropatches over a voltage range between −100 to +250 mV using an intracellular Ca^{2+} concentration of about 40 nM revealed a leftward shift in the voltage-activation curves in macropatches expressing BK_{G354S} compared with BK_{WT}. However, at a 100 μM internal Ca^{2+} concentration, both mutant and BK_{WT} have similar voltage dependence and half-activation voltages (Fig. 3*C*). Both the BK_{WT} and BK_{G354S} are sensitive to Ca^{2+}; however, the smaller Ca^{2+}-induced leftward shift of the G–V in the mutant suggests that its apparent Ca^{2+} sensitivity is less than that of the WT BK, further exacerbating the LOF phenotype. Noise analysis of the K^+ conductance revealed a single-channel conductance of only 13.2 ± 1.5 pS (n = 5), a dramatic decrease compared to the single-channel conductance of around 180 to 200 pS from BK_{WT} in symmetrical 110 mM K^+ (Fig. 3*D*). Notably, the 13 pS we found for K^+ conductance of BK_{G354S} is 6.5% of that of BK_{WT} (203 pS), which is a value very close to the 5.5% estimated with macroscopic currents from the cut-open oocytes experiments (*SI Appendix*, Fig. S1).

We also compared the K^+ selectivity of BK_{G354S} with BK_{WT} by recording voltage-activated currents in symmetrical condition (140 mM K^+ in both sides of the membrane) and under biionic condition (140 mM Na^+ in the intracellular side and 140 mM K^+ in the extracellular side of the membrane). The reversal potential was zero in symmetrical condition for both BK_{WT} and BK_{G354S} (Fig. 4 *A* and *B*, upper traces, and Fig. 4 *C* and *D*, K_{ext}/K_{int}). Under biionic condition, the reversal potential was undetermined for BK_{WT} (greater than +100 mV [n = 3]) and +40 ± 3 mV (n = 3) for BK_{G354S} (Fig. 4 *A* and *B*, lower traces, and Fig. 4 *C* and *D*, K_{ext}/Na_{int}). These data confirm previous results showing no measurable permeation can be detected for Na^+ in the case of the BK_{WT}. From the reversal potential for the BK_{G354S} channel in biionic condition, we calculated a PK^+:PNa^+ ratio of 4.8 (Fig. 4; *Materials and Methods*). This result indicates a considerable loss of K^+ selectivity in BK_{G354S}, and it agrees with the loss of selectivity caused by the analog mutation in the Shaker K^+ channel selectivity filter (31).

Recording of BK_{G354S} Expressed in HEK Cells. Additionally, we used the HEK cell system to express and compare BK_{WT} and BK_{G354S} channels. These electrophysiological experiments were particularly important since HEK cells are a human cell line. Consistent with the reduction of K^+ currents seen when BK_{G354S} was expressed in *Xenopus* oocytes, macroscopic currents recorded in inside-out patches on cells expressing BK_{G354S} showed a reduction in the macroscopic K^+ currents compared to cells expressing BK_{WT} (Fig. 5 *A* and *B*). Also confirming the oocytes experiments, the voltage activation curve for the BK_{G354S} mutant at 40 nM Ca^{2+} was leftward shifted by approximately −51 mV (Fig. 5*C*). More importantly, the single-channel conductance of the mutant channel (10 ± 2 pS) as determined by noise analysis was dramatically reduced compared to that of the BK_{WT} channel (172 pS; cf. Fig. 5 *D* and *E*).

Taken together, our functional results strongly suggest that mutation G354S in BK channels induces a LOF by decreasing the unitary conductance of the channel, and by a loss of selectivity to K^+. The data also show that the reduction in G354S

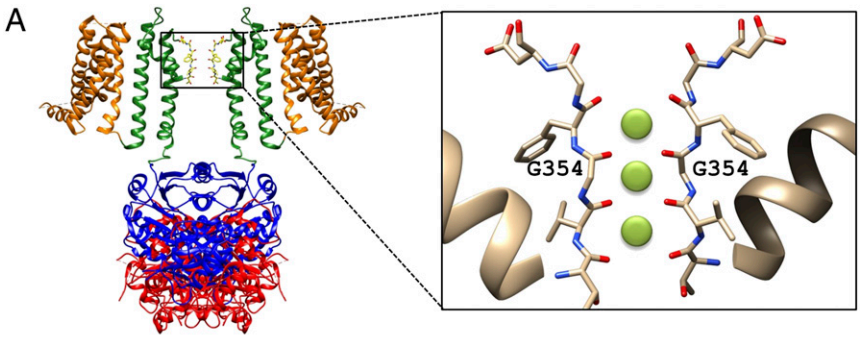

B

HUMAN	-TMSTV**G**YGDVY-
MOUSE	-TMSTV**G**YGDVY-
RAT	-TMSTV**G**YGDVY-
BOVIN	-TMSTV**G**YGDVY-
RABBIT	-TMSTV**G**YGDVY-
CHICKEN	-TMSTV**G**YGDVY-
XENOPUS	-TMSTV**G**YGDVY-
DROSOPHILA	-TMSTV**G**YGDVY-
APLYSIA	-TMSTV**G**FGDIF-

C

KCNA1_HUMAN	-SMTTV**G**YGDVY-
KCNB1_HUMAN	-TMTTV**G**YGDIY-
KCNC1_HUMAN	-TMTTL**G**YGDMY-
KCND1_HUMAN	-TMTTL**G**YGDMV-
KCNQ1_HUMAN	-TVTTI**G**YGDKV-
HCN1_HUMAN	-HMLCI**G**YGAQA-
KCNMA1_HUMAN	-TMSTV**G**YGDVY-
KCNH1_HUMAN	-SLTSV**G**FGNIA-
KCNH2_HUMAN	-SLTSV**G**FGNVS-

Fig. 2. The G354S mutation is located in the highly conserved signature sequence "TVGYG" of potassium channels. (*A*, *Left*) Side view of two *Aplysia* BK subunits from structural studies by cryo-EM (Protein Data Bank [PDB]: 5TJ6). Color code: voltage-sensor domain (orange), pore domain (green), RCK1 domain (blue), and RCK2 domain (red). (*A*, *Right*) Close view of the selectivity filter with the G354 annotated. (*B*) TVGYG in *KCNMA1* is conserved among species with TVGFG sequence in *Aplysia*'s BK channels instead of TVGYG in all other species shown. (*C*) The selectivity filter G354 residue from the BK channel is also conserved in the α-subunits of other human K^+-selective channels.

macroscopic currents is mainly due to the decrease in single-channel conductance and not to reduced channel expression. Moreover, our data from BK_{WT} and BK_{G354S} channels expressed together in oocytes suggest that BK_{G354S} protein exerts a dominant-negative effect when coassembled with BK_{WT} in the same heterochannel (*SI Appendix*, Fig. S1).

NS1619 is a synthetic benzimidazole derivative, and it is a specific BK channel activator in the micromolar range (22). The compound produces a reversible dose-dependent leftward shift antagonized by the scorpion toxin charybdotoxin. Gessner et al. (32) proposed that NS1619 activates BK channels by interacting with the S6/RCK1 linker. Fig. 6 *A*–*C* shows that NS1619, as reported previously, robustly activates BK_{WT} in HEK cell. Conversely, we found that the NS1619 behaves as a potent antagonist of the BK_{G354S} mutant channel (Fig. 6 *D*–*F*).

The BK_{G354S} Mutation Reduces Neurite Outgrowth. To investigate the effect of the BK_{G354S} mutation on differentiation in cultured mammalian cells, we transfected BK_{WT} or BK_{G354S} into PC12 cells, which undergo differentiation into neuronal phenotype in response to nerve growth factor (NGF). Upon induction with NGF for 24 and 48 h, we observed a significantly reduced total neurite length in cells expressing BK_{G354S} channel compared to BK_{WT} in 48 h (Fig. 7 *A*–*C* and *F*). The percentage of cells bearing neurites was similar between cells expressing BK_{WT} and BK_{G354S} channels (Fig. 7 *B*, *C*, and *E*). To test whether reduced neurite outgrowth of the PC12 cells expressing the BK_{G354S} channel could be attributed to BK channel function, we incubated cells in the BK channel activator NS1619. The neurite outgrowth in a PC12 cell expressing BK_{G354S} channels was improved after treatment with NS1619 at 30 μM, although it did not reach normal values (Fig. 7*D*). The average NGF-induced neurite length for cells expressing BK_{G354S}, compared to BK_{WT}, was increased 18.87 ± 2.31% after 24 h with NS1619 and 29.20 ± 3.12% after 48 h with NS1619 (cf. Fig. 7 *F* and *G*).

The BK_{G354S} Mutation Reduces Cell Viability. When assessed by flow cytometry, PC12 cells expressing BK_{G354S} exhibited 1.6-fold greater degree of cell death compared to cells expressing BK_{WT} (Fig. 7 *H* and *I*). To test whether the reduced viability of the PC12 cells expressing the mutant channel could be attributed to BK channel function, we incubated cells in the BK channel activator NS1619. Cell death associated with BK_{G354S}-expressing cells was corrected by pretreatment of cells with NS1619 at 30 μM and was similar to control BK_{WT} cells (Fig. 7 *H* and *I*); the similar data were obtained from HEK cells.

Since BK_{G354S} is toxic when expressed in HEK or PC12 cells that express native endogenous BK channels, we hypothesized that toxicity of the low-conductance BK_{G354S} mutant may result from a dominant-negative effect, eliminating critical endogenous ordinary BK channel currents. Alternatively, the altered ion selectivity of the BK_{G354S} mutant may disrupt Na^+ concentration gradient, leading to loss of membrane potential. In either case, these results suggest that normal BK channel activity is important for the viability of these cultured cells. To test this, we used siRNA specific for BK channel α-subunit, the *KCNMA1* gene product of BK channels, to knock down endogenous BK channels in PC12 cells, and compared the viability of PC12 cells between siRNA*KCNMA1* and siRNA*Control*. Interestingly, cells depleted of their endogenous BK channels exhibited increased cell death compared to control cells and comparable to those transfected with the mutant BK_{G354S} (Fig. 7 *H* and *I*); however, NS1619 was not able to rescue the cells treated with siRNA*KCNMA1*. This result suggests that, in cultured cells, cellular viability is dependent on the presence of normal BK channel function. The protection by NS1619 may result from either activation of endogenous BK channels or the selective blockade of the BK_{G354S} mutant channels, or, most likely a combination of the two effects.

The BK_{G354S} Mutation Traffic to Plasma Membrane and Mitochondria. Many ion channel mutations affect subcellular trafficking or membrane insertion of the channel proteins. BK channels are normally present on multiple subcellular organelles in addition to the plasma membrane. To test whether BK_{G354S} mutant and BK_{WT} channels localize equally in the plasma membrane and other organelles, we subjected transfected cell lysates to subcellular fractionation and analysis by immunoblotting using HEK cells. The 100-kDa BK channel polypeptides were found present in the plasma membrane fraction of untransfected and to an increased, but equivalent extent in cells transfected with either BK_{G354S} or BK_{WT} plasmids (Fig. 8 *A* and *C*). Also, there was a detectable 100-kDa polypeptide present in mitochondrial fractions

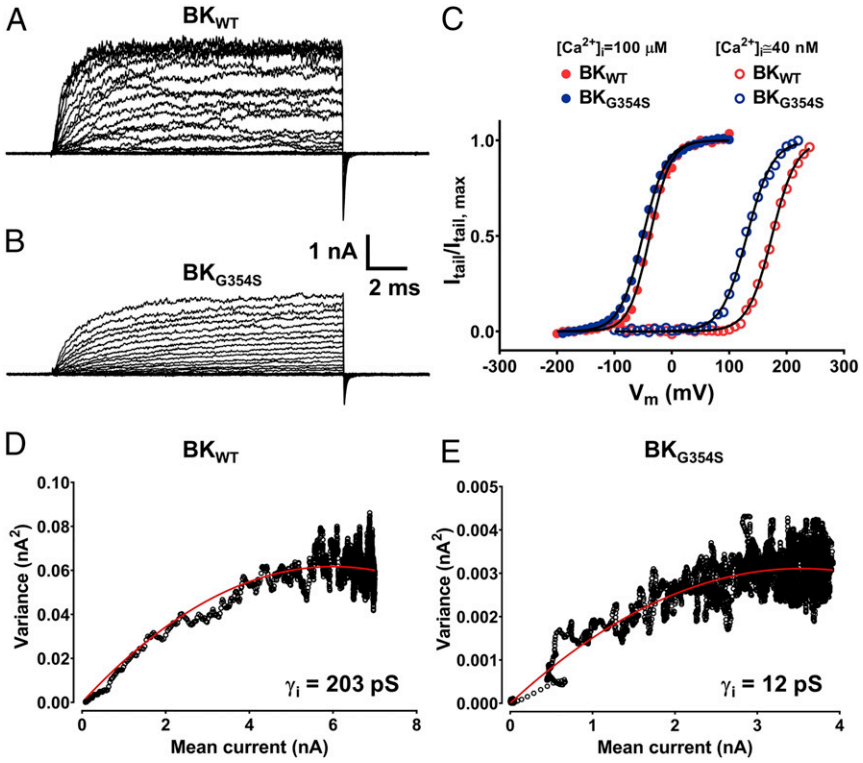

Fig. 3. Characterization of BK_{G354S} mutant ionic currents. (*A*) Representative BK_{WT} ionic currents evoked by voltage steps from −200 to +250 range in 10-mV steps. Holding potential was −100 mV and the records made in nominal absence of internal Ca^{2+} (≅40 nM Ca^{2+}). (*B*) BK_{G354S} macroscopic currents in the same conditions as in *A*. (*C*) Relative tail currents vs. voltage [$(I_{tail}/I_{tail,max})$–*V*] curves were obtained from experiments with ≅40 nM internal Ca^{2+} (as those shown in *A* and *B*; black circles) and at 100 μM Ca^{2+} (red circles). Continuous lines are best fits to the data using Eq. 2 (*SI Appendix, SI Materials and Methods*). For the BK_{WT} channel, parameters were (mean ± SEM): $V_{1/2}$ = 174 ± 3 mV, z = 1.21 ± 0.05 at $[Ca^{2+}]_i$ = 40 nM, n = 10; $V_{1/2}$ = −38 ± 6 mV, z = 1.41 ± 0.03 at $[Ca^{2+}]_i$ = 100 μM, n = 7. For the BK_{G354S} channel, parameters were (mean ± SEM): $V_{1/2}$ = 131 ± 3 mV, z = 1.14 ± 0.03 at $[Ca^{2+}]_i$ = 40 nM, n = 10; $V_{1/2}$ = −50 ± 4 mV, z = 1.24 ± 0.04 at $[Ca^{2+}]_i$ = 100 μM, n = 6. (*D* and *E*) Representative nonstationary noise analysis of BK_{WT} and BK_{G354S} currents, respectively. Inside-out patches were held at 0 mV and pulsed 200 times to 250 mV (BK_{WT}) or 150 mV (BK_{G354S}) during 10 ms. The intracellular (bath) solution was formulated for a Ca^{2+} concentration of 40 nM. The red lines are a fit to the data using Eq. 3 (*SI Appendix, SI Materials and Methods*). For BK_{WT} (*D*), considering a 250 mV driving force (the experiment was done in symmetrical K^+) and i = 50.8 pA, the patch had an average single-channel conductance (γ_i) of 203 pS. For BK_{G354S} (*E*), γ_i was reduced compared with that of the WT channel with a value of 12 pS (i = 1.8 pA and 150 mV of driving force).

in both untransfected cells and cells transfected with BK_{G354S} and BK_{WT} constructs (Fig. 8 *B* and *C*).

To characterize the subcellular distribution of the BK_{G354S} and BK_{WT} channels morphologically, we examined HEK and PC12 cells transiently transfected with BK_{WT} or BK_{G354S} channels by immunofluorescence labeling using BK channel-specific antibodies. HEK cell transiently expressing either BK channel displayed diffuse membrane fluorescence with no pattern difference between BK_{G354S} or BK_{WT} channels (Fig. 8*H*). Colocalization analysis using mitochondrial probe MitoTracker Red also showed that both BK_{WT} and BK_{G354S} channels are expressed in mitochondria, although, as described below, at different levels (Fig. 8*H*).

The BK_{G354S} Mutation Causes Selective Toxicity to Mitochondria. We noticed that the intensity of the 100 kDa band in the mitochondria was consistently lower in cells expressing the BK_{G354S} compared with BK_{WT} when normalized to cellular GAPDH protein (Fig. 8*C*). To investigate whether this reduction was due to selective loss of BK channels in mitochondria, we compared the signal for the mitochondrial voltage-dependent anion channel (VDAC), as a marker for the mitochondrial compartment. The signal for VDAC was also consistently reduced by 50% relative to cells transfected with the BK_{WT} channel or pcDNA3 control as assessed by immunoblotting (Fig. 8 *B* and *C*). However, when we normalized the BK_{WT} or BK_{G354S} levels in the mitochondrial fraction to the VDAC protein signal in the same fractions, there was no difference between cells expressing the BK_{WT} or BK_{G354S} mutant channel (Fig. 8 *B* and *C*). This suggests that, rather than selective mitochondrial loss of BK channels in cells expressing BK_{G354S}, the mutation itself leads to a reduction in mitochondrial content. To test whether the effect of BK_{G354S} on normal BK channel currents indicated a critical dependence of mitochondria on BK channels, we used siRNA *KCNMA1* in HEK cells to knock down BK channels. Genetic silencing of BK channels led to reduced BK channels both in the membrane and mitochondrial fractions (Fig. 8 *A*–*C*).

In addition, knockdown of endogenous BK channels was also accompanied by a decrease in the amount of VDAC protein in cells, supporting the idea that loss of BK channel activity reduced mitochondrial content (Fig. 8 *B* and *C*). To determine whether BK mutation affects components of the mitochondrial respiratory pathway, we examined several proteins of electron transport chain complexes. Levels of Complex I subunit NDUFB8, Complex II subunit, Complex III subunit Core 2, Complex IV subunit II, and ATP synthase subunit α, all components of the mitochondrial oxidative phosphorylation metabolic pathway (OXPHOS), were decreased in cells expressing BK_{G354S} relative to BK_{WT}-expressing cells (Fig. 8 *F* and *G*).

To compare the subcellular distribution of BK_{G354S} and BK_{WT} in mitochondria, we transiently transfected HEK cells, because of their superior resolution of subcellular compartments. We stained cells expressing BK_{WT} or BK_{G354S} with Tommo20 for mitochondria (red) and immunolabeled BK channels with anti-BK channel antibody (green). Fig. 8 *H* and *I* shows that the intensity of mitochondrial labeling was decreased in BK_{G354S}-expressing cells compared with BK_{WT}-expressing cells. Colocalization of Tommo20 and BK channel antibody also revealed a significantly lower immunolabeling signal in BK_{G354S} than that in BK_{WT} (Fig. 8 *H* and *I*).

Furthermore, silencing of BK channels using siRNA *KCNMA1* led to a reduction of the mitochondrial labeling intensity for Tommo20 compared with siRNA *Control* (*SI Appendix*, Fig. S2 *E* and *F*).

Finally, to test whether the reduced mitochondrial content was related to BK channels affected by the presence of BK_{G354S} subunit(s), we also treated cells transiently expressing BK_{WT} or BK_{G354S} channels with NS1619, known to improve neurite outgrowth and protect from cell death in cells expressing BK_{G354S} channels. Fig. 8*D* shows that pretreatment of HEK cells expressing BK_{G354S} channels with NS1619 protected the reduction of mitochondrial VDAC protein. However, treatment with NS1619 could not protect cells and prevent reduction of mitochondrial content in cells treated with *KCNMA1*-specific siRNA (Fig. 8 *D* and *E* and *SI Appendix*, Fig. S2 *B* and *C*). This suggests that mutation in BK_{G354S} specifically affects channel function, and a drug acting as NS1619 might be protective in some ataxia patients.

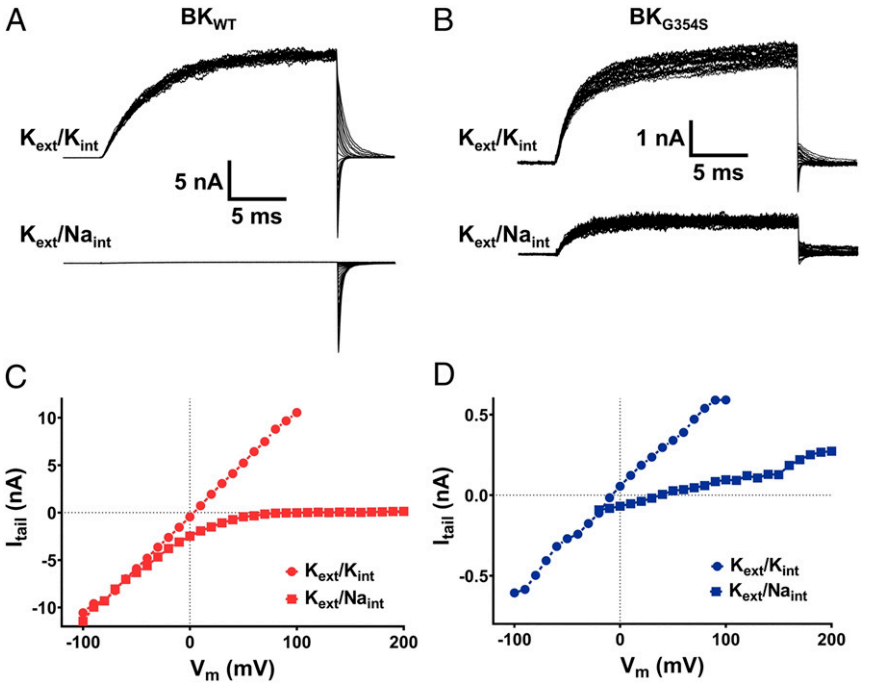

Fig. 4. The BK_{WT} channel and the BK_{G354S} mutant channel display different selectivity. Raw current traces from BK_{WT} (*A*), or BK_{G354S} channels (*B*), from either 140 mM K^+ or 140 mM Na^+ in the internal (bath) solution. Currents were recorded from excised, inside-out membrane patches, with 140 mM K^+ in the extracellular (pipette) solution. Currents were activated by a step to 200 mV, followed by voltage pulses ranging from 200 to −100 mV (100 to −20 mV for the mutant), in 10-mV decrements. Leak and capacitive currents were subtracted using a P/-8 subtraction protocol (53). (*C* and *D*) Isochronal I_{tail}–*V* curves were taken from the records shown in *A* and *B*, respectively, in the presence of internal K^+ (K_{ext}/K_{int}, circles) or Na^+ (K_{ext}/Na_{int}, squares), to determine the reversal potential for each case.

Mitochondria Ultrastructure Is Disrupted by the BK_{G354S} Mutation. We performed electron-microscopic (EM) image analysis of mitochondrial content and ultrastructure in stably expressing BK_{WT} and BK_{G354S} cells (Fig. 9 *A*–*C*). Mitochondria in BK_{G354S}-expressing cells are fewer in number (Fig. 9*C*) and have abnormal-appearing cristae compared with BK_{WT} and pcDNA3-expressing cells (Fig. 9*B*). Quantification reveals a 58.89 ± 4.62% reduction in mitochondrial number in BK_{G354S}-expressing cells compared with BK_{WT} and pcDNA3-expressing cells. In addition, 44.36 ± 4.78% of mitochondria have distended and disordered cristae in BK_{G354S} stable expressing cells (Fig. 9*C*).

Mitochondria Dynamics Change and Potential Decreased in Live BK_{G354S} Mutation Cells. To observe dynamic changes of mitochondrial fusion and fission affected by the BK_{G354S} mutation, we used MitoTracker Red, to stain live PC12 cells stably expressing BK_{WT}, BK_{G354S}, or pCDNA3. Live-cell imaging indicated grossly reduced content of mitochondria in cells expressing the BK_{G354S} mutation (Movies S5 and S6) compared with cells expressing BK_{WT} and control (Movies S1–S4). Elongated and interconnected fusion mitochondrial forms are predominant in cells expressing BK_{WT} and control. In contrast, fragmentated fission forms are more prevalent in cells expressing the BK_{G354S} mutation.

To investigate whether the BK_{G354S} affects mitochondrial membrane potential in addition to its effect on mitochondrial fusion and fission, we used fluorescent probes TMRM and MitoTracker green to monitor the mitochondrial membrane potential in BK_{G354S} stably expressing cells compared with BK_{WT} and pcDNA3 stably expressing cells (Fig. 9 *D*–*F*). The integrated intensity of TMRM/MitoTracker was decreased 43.5 ± 3% in BK_{G354S} stably expressing cells compared to BK_{WT} and pcDNA3 stably expressing cells (Fig. 9*F*). NS1619 treatment of BK_{G354S} stably expressing cells was able to rescue the integrated intensity of TMRM/MitoTracker to 81.4 ± 4.4% that of control. Thus, NS1619 restored the membrane potential in a significant number of mitochondria in cells expressing BK_{G354S}. These results indicate that impaired gating of the BK_{G354S} mutation is directly responsible for depolarized or dysfunctional mitochondria.

BK_{G354S} Causes Ataxia in Mice. Because mice with targeted deletion of the BK channel α-subunit develop ataxia, we hypothesized that the LOF BK channel mutation acts in a similar fashion. To test for a direct effect of BK_{G354S} on cerebellar function, we engineered adenoassociated virus 9 (AAV9)-based expression vectors to deliver BK_{WT} or mutant BK_{G354S} channels to neonatal mice. We injected 2 μL at 1×10^{12} vg/μL of AAV9-BK_{WT} or AAV9-BK_{G354S} into mouse intracerebroventricularly at postnatal day 0 (P0) (33). Mice tolerated the injections well and developed normally with no visible neurological deficits initially. Analysis of the histological features of the cerebellar cortex shows no obvious difference between mice injected with BK_{G354S} vs. BK_{WT} channel, a finding similar to that of BK knockout mice. To investigate whether the mutant BK channel expression affects motor function, AAV9-BK_{WT}– or AAV9-BK_{G354S}–treated mice were studied on a motorized treadmill equipped with a high-speed digital camera (DigiGait) (Mouse Specifics) (34) at 40 and 80 d of age to quantitatively assess 20 gait and limb movement parameters, for both left and right sides and both forelimb and hindlimb. After post hoc correction, significant abnormalities of motor temporal and spatial parameters, either unilaterally or bilaterally, were seen at P40 in 42% and at P80 in 55% of parameters. From these parameters, an ataxia coefficient is generated by DigiGait software. The coefficient of ataxia increased from 11.45 ± 1.4% and 8.7 ± 2.4% to 40.78 ± 2.3% and 52.36 ± 3.3% for both left and right hindlimbs, respectively, in AAV9-BK_{G354S} mice from 40 to 80 d of age (*SI Appendix*, Fig. S3). *SI Appendix*, Fig. S3 displays representative plots gait parameters that were significantly different and impaired in the mice receiving BK_{G354S} compared to those injected with BK_{WT}. These findings

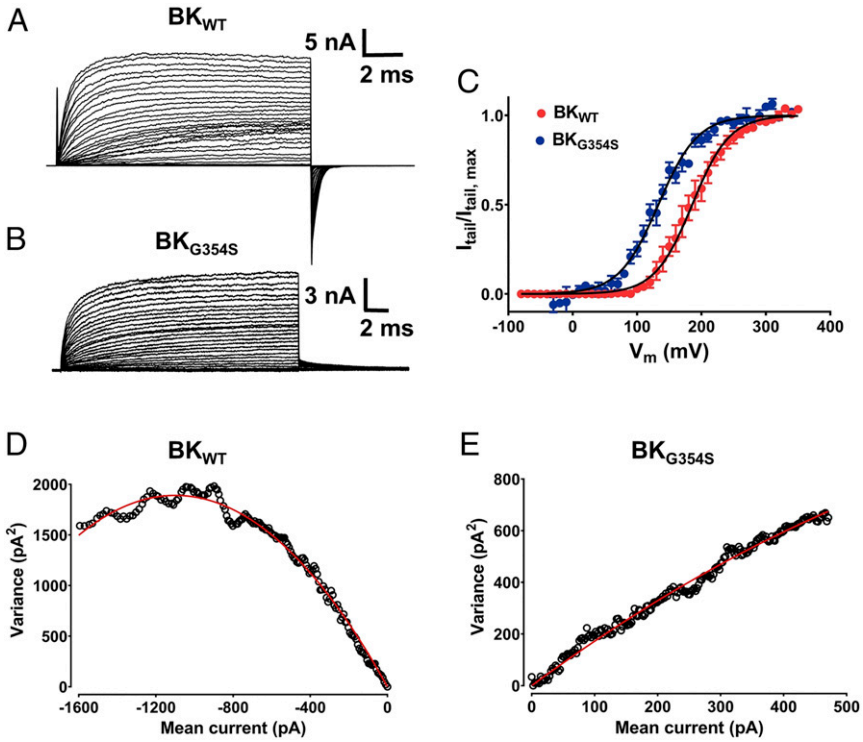

Fig. 5. Characterization of BK_{WT} and BK_{G354S} ionic currents in HEK cells. (*A*) Macroscopic K^+ currents in an inside-out membrane patch expressing BK_{WT} channels. BK_{G354S} currents were evoked by voltage steps from −120 to 350 mV from a prepulse of −80 in 10-mV steps returning to −80 mV. The holding potential was 0 mV. (*B*) BK_{G354S} macroscopic currents elicited by voltage pulses from 0 to 330 mV in 10-mV steps, returning to 60 mV. The stimulation protocol consisted of a prepulse of −80 mV, followed by voltage pulses in the range of 0 to 330 mV with increments every 10 mV, returning to 60 mV. (*C*) Normalized tail currents ($I_{tail}/I_{tail,max}$) vs. voltage data. The solid lines are the best fit to the data using Eq. 2 (*SI Appendix, SI Materials and Methods*). For the BK_{WT} channels, parameters were as follows (mean ± SEM; $n = 3$ [red]): $V_{1/2} = 185 \pm 16$ mV, $z = 0.88 \pm 0.02$; BKα G354S, $n = 7$. For the BK_{G354S}, parameters were as follows (mean ± SEM; $n = 7$ [blue]): $V_{1/2} = 134 \pm 16$ mV, $z = 0.84 \pm 0.03$. All data were obtained in the nominal absence of Ca^{2+}. (*D*) Representative nonstationary noise analysis of BK_{WT} macroscopic currents. The patch was held at −80 mV and pulsed 200 times at 200 mV taken in the tail. The stimulation protocol consisted of a prepulse of −80 mV, followed by 200 pulses of 200 mV, returning to −20 mV. Noise analysis was done using the tail currents. Holding potential was 0 mV. The patch had 6,110 active channels with an average single-channel conductance of 172 pS. The average single-channel conductance was 170 ± 3 pS ($n = 7$). (*E*) Representative nonstationary noise analysis of G354S mutant macroscopic currents. Currents were evoked using a prepulse of −80 mV, followed by 200 pulses of 130 mV, returning to 60 mV. Noise analysis performed using the K^+ currents elicited by the 130-mV pulses. The patch had 2,180 active channels with an average single-channel conductance of 9 pS. The average single-channel conductance was 10 ± 2 pS ($n = 5$).

directly implicate the role of this mutant channel in the clinical manifestations of ataxia in these mice.

SK/BK Channel Activator Improves Coordination in the Patient. Potassium channel-activating drugs have recently shown some benefit in treating ataxia (35, 36). Presently, there are not pure BK channel activators approved for use in patients by the Food and Drug Administration. Chlorzoxazone is a mixed SK/BK channel activator marketed under the name Parafon Forte. We assessed the effects of this drug on motor performance in this patient. The patient was assessed semiquantitatively using the Scale for Assessment and Rating of Ataxia (SARA) rating scale by three examiners before treatment, two of whom were "blinded" as to treatment. The mean SARA score of this patient was 20.7 before the initiation of therapy (*SI Appendix*, Table S3). Also, the balance and truncal stability of the patient were evaluated using a computerized dynamic posturography (CDP) apparatus by an examiner who was blinded as to treatment, which assesses sway under six conditions (37). The patient was subsequently started on chlorzoxazone, 500 mg QID, and returned after 1 mo of therapy. Repeat SARA testing revealed a mean score of 18.3. Repeat CDP showed an ∼10% improvement in the composite score with a marked improvement in condition 3, in which the patient relies only on proprioceptive and vestibular cues. Unfortunately, follow-up after 6 mo on the medication revealed continued disease progression. Our results suggest that activation of endogenous SK and BK channels in these BK mutant patients may provide symptomatic improvement. Continued disease progression in this case may indicate that chlorzoxazone has no effect on blocking the mutant BK_{G354S} channel (*SI Appendix*, Fig. S4).

Discussion

The diversity of genetic and mutational defects identified for SCAs suggests that multiple pathophysiological mechanisms lead to a common clinical and pathological phenotype. The numerous ion channel mutations implicated in the ataxias indicate that disturbances of intracellular ionic milieu might be a frequent pathophysiological mechanism affecting Purkinje cells (1–4, 6, 38–41). However, the pathogenic mechanisms coupling disturbed membrane ionic flux to pathological changes at the cellular and subcellular level remain to be elucidated. Previous studies have shown that expression of mutant *KCND3*-encoded channels ($K_V4.3$) from SCA19 ataxia patients in cultured Purkinje cells reduces viability and dendritic outgrowth (42). In the present study, we demonstrate that a spontaneously occurring mutation in *KCNMA1*-encoded channels (BK), predicting an amino acid change in the selectivity filter of the channel, leads to the LOF of the BK channel phenotype with severely reduced channel conductance with loss of K^+ selectivity. In addition, the patient affected by this mutation presents a syndrome of progressive cerebellar ataxia, cognitive impairment, and dyskinesia. At least seven other reported *KCNMA1* LOF mutations are associated

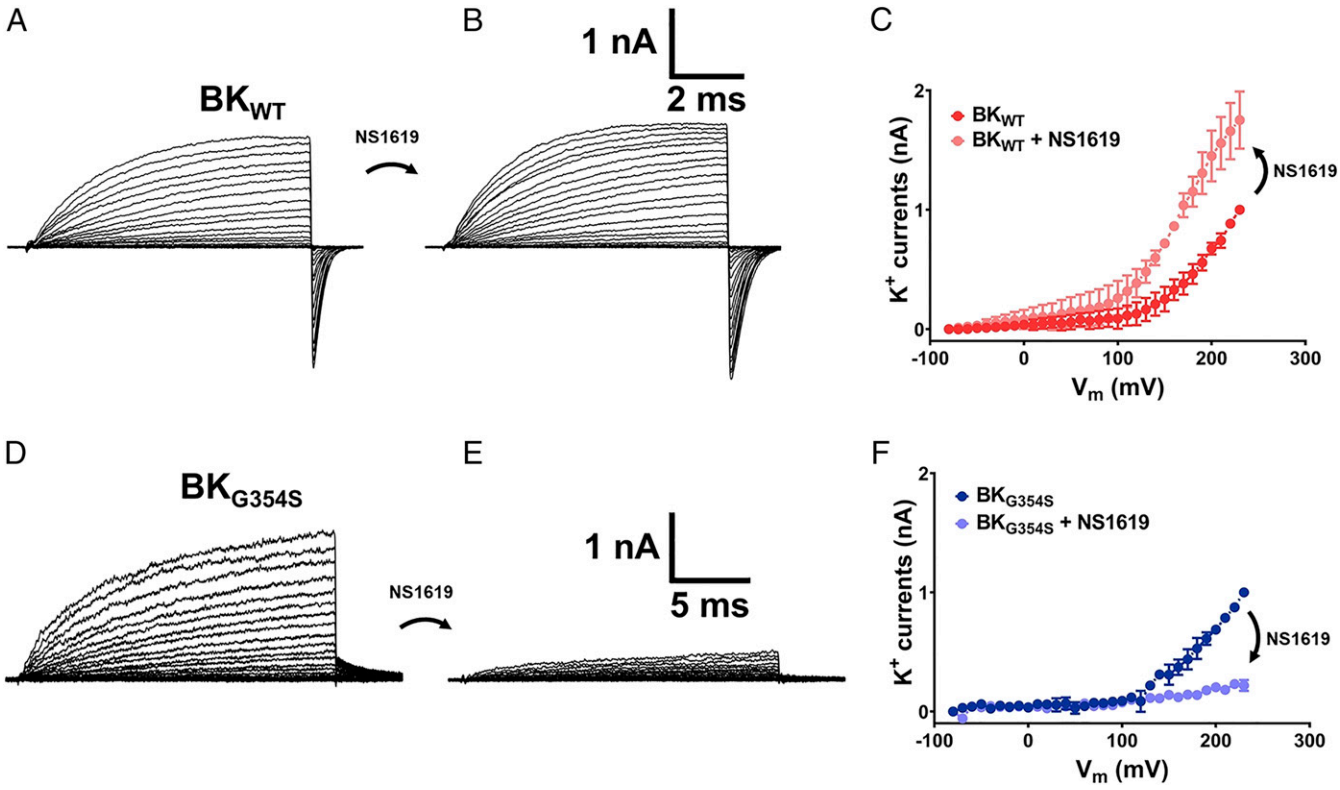

Fig. 6. Effect of NS1619 on BK_{WT} and BK_{G354S} macroscopic currents. (*A*) BK_{WT} macroscopic currents. The voltage protocol consisted of a prepulse of −80 mV, followed by voltage pulses in the range of −80 to 250 mV with increments every 10 mV, returning to −80 mV. The holding potential was 0 mV. (*B*) BK_{WT} macroscopic currents in the presence of NS1619 added to a final concentration of 10 μM. The stimulation protocol consisted of a prepulse of −80 mV, followed by voltage pulses in the range of −80 to 250 mV with increments every 10 mV, returning to −80 mV. The holding potential was 0 mV. BK_{WT} DNA transfected 250 ng/μL. (*C*) BK_{WT} currents vs. voltage (*I/V*) curve (red) and BK_{WT} currents vs. voltage (*I/V*) curve in the presence of 10 μM NS1619 (light red; $n = 3$). (*D*) BK_{G354S} macroscopic currents. The voltage protocol consisted of a prepulse of −80 mV, followed by voltage pulses in the range of −80 to 230 mV with increments every 10 mV, returning to 60 mV. The holding potential was 0 mV. (*E*) BK_{G354S} macroscopic currents in the presence of 10 μM NS1619 added to a final concentration of 10 μM. (*F*) BK_{G354S} current vs. voltage curve (blue) and BK_{G354S} current vs. voltage curve in the presence of 10 μM NS1619 (light blue). The voltage protocol consisted of a prepulse of −80 mV, followed by voltage pulses in the range of −80 to 230 mV with increments every 10 mV, returning to 60 mV. BK_{G354S} DNA transfected 450 ng/μL.

with cerebellar impairment, and two others with cognitive impairment (13). Moreover, AAV-mediated delivery of the BK_{G354S} channel, but not the BK_{WT} channel, produced ataxic gait in mice. Genetic ablation of the *KCNMA1* also led to ataxia in mice. Together, these observations indicate a strong dependency of cerebellar function on normal BK channel activity.

BK channels are similar to other voltage-gated potassium channels in that they contain a highly conserved 352-TVGYG-356 sequence in the pore-forming domain known as the selectivity filter (Fig. 3), precisely the moiety where the G354S mutation is predicted in the present patient. It is instructive that other spontaneous mutations in the BK channel lead to enhanced rather than reduced BK channel activity and have a distinct clinical picture. D434G (BK_{D434G}), within the RCK domain, is a GOF mutation yielding a channel that is more sensitive to Ca^{2+} and that opens faster and at more negative voltages (14). N995S (BK_{N995S}) is a GOF mutation reported in three individuals causing a leftward shift of the conductance–voltage (*G–V*) curve. The GOF mutations are not associated with ataxia or cerebellar atrophy, but instead have been associated with epileptic syndromes and paroxysmal dyskinesia.

A full assessment of the probable heterotetramerization of BK_{WT} and BK_{G354S} subunits in the same channel is beyond the scope of this study. In our preliminary results, unitary currents studied by both single-channel patch clamp and by noise analysis of macroscopic currents in membranes from oocytes injected previously with cRNA for both types of proteins, never showed intermediary conductance. On the other hand, macroscopic K^+ currents recorded from these cells showed evidence of heterotetramerization. First, BK_{WT} expression, as measured by the amplitude of the macroscopic K^+ currents, was affected by the likely coexpression, in the same oocyte, of BK_{G354S}, suggesting dominant-negative effect and in agreement with the mitochondrial studies. Second, the time constants of the putative $BK_{WT\text{-}G354S}$ activation kinetics sit in between the BK_{WT} and BK_{G354S} values. Third, the voltage dependence of the activation kinetics resembles that of pure BK_{G354S} channels: They are virtually voltage independent (*SI Appendix*, Fig. S1).

An important aspect of this BK_{G354S} channel phenotype is that it conducts Na^+ with the permeability of ∼20% of the K^+ permeability. This BK_{G354S} channel Na^+ permeability may play an important role in the clinicopathological phenotype since during neuronal activity BK channels normally act by damping excitatory processes mediated by an increase in internal Ca^{2+}. In other words, the increased Na^+ permeability may be as significant a deleterious property of this mutant channel as the dramatic depression of the K^+ conductance. The mutant channel therefore should conduct Na^+ inwardly when activated, producing longer periods of depolarization. Under physiological intracellular and extracellular concentrations of Na^+ and K^+, the current carried by these mutant channels has a reversal potential near −40 mV, and therefore the BK_{G354S} effect on the membrane potential is toward keeping it near −40 mV, most likely above the threshold voltage for action potential generation by neurons. Thus, we hypothesize that when the plasma membrane

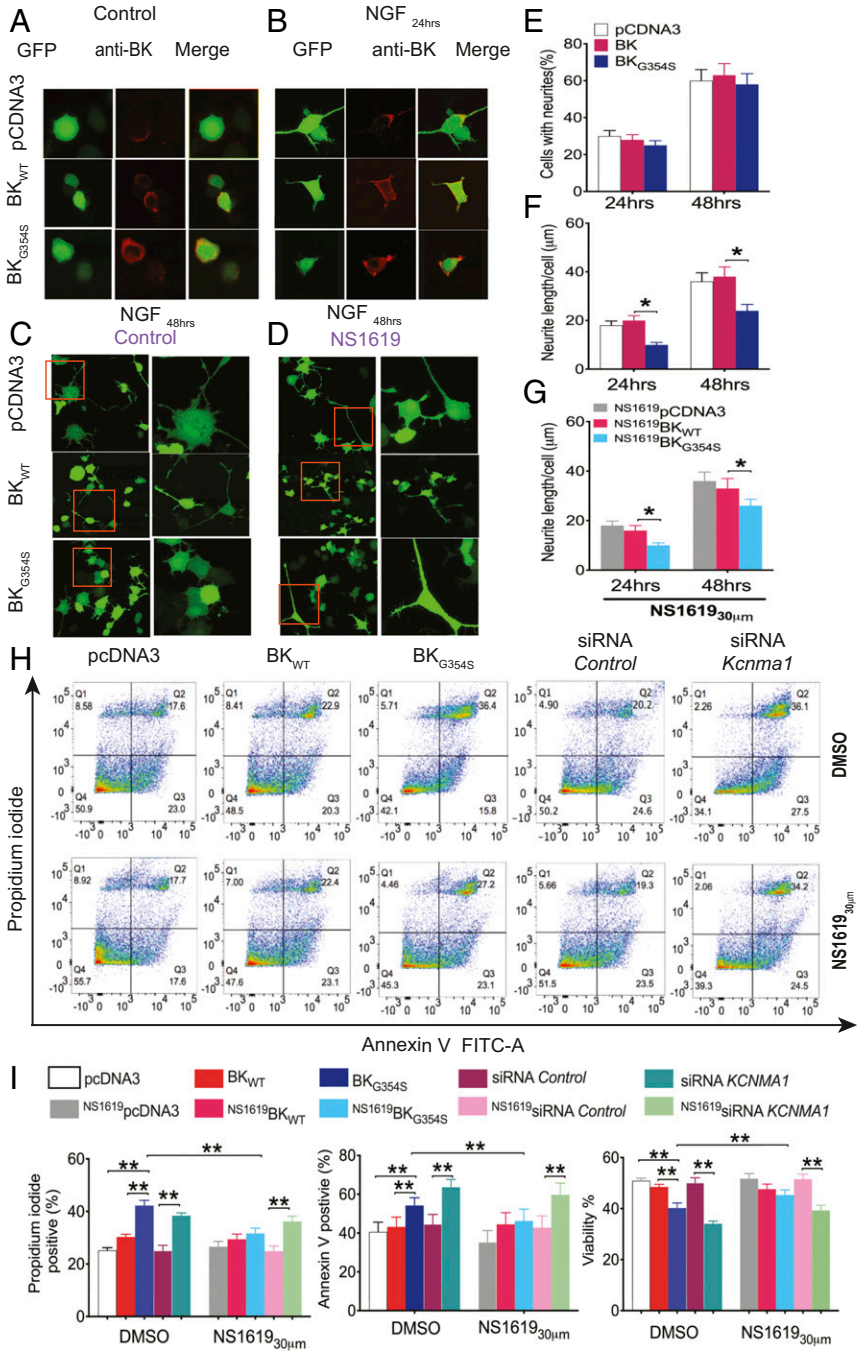

Fig. 7. Cells expressing the mutant BK_{G354S} channel have reduced neurite outgrowth and cell viability, which is rescued by NS1619. (*A* and *B*) Both BK_{WT} and BK_{G354S} channels locate on the cell membrane in the representative confocal images with or without NGF stimulation. Detectable BK labeling can be seen in PC12 pCDNA3-only transfection because of possible endogenous expression. After 24 h in the presence of NGF, no neurites are present in cells expressing the mutant, although a systematic check shows no difference between cells expressing BK_{WT} or BK_{G354S}. Quantitative analysis of data present in *E* and *F*. (*C* and *D*) Representative low- and high-magnification images of PC12 cells transiently cotransfected pEGFP with pcDNA3, BK_{WT}, and BK_{G354S} channels at 48 h with NGF induction with (*C*) or without (*D*) NS1619 treatment. (*E*–*G*) Quantitation of average percentage of neurites per cell and neurite length ($n \geq 6$; $^*P < 0.05$; $^{**}P < 0.01$). (*H*) Representative fluorescence dot blots of FITC-Annexin V and propidium iodide (PI). PI-stained HEK cells transiently transfected with pcDNA3, BK_{WT}, or BK_{G354S} channels without (*Upper* row) or with (*Lower* row) 30 μM NS1619 treatment ($n \geq 6$; $^*P < 0.05$; $^{**}P < 0.01$). (*I*) Quantitation of FITC-Annexin-V– and PI-positive cells and cell viability in PC12 cells transiently transfected with pcDNA3, BK_{WT}, or BK_{G354S} channels without (*Upper* row) or with (*Lower* row) 30 μM NS1619 treatment ($n \geq 6$; $^*P < 0.05$; $^{**}P < 0.01$).

BK_{G354S} channel is activated it should act by increasing neurotransmitter release and should not be able to modulate action potential duration adequately.

The unexpected blocking effect of NS1619 on the BK_{G354S} conductance (to K^+ and more importantly to Na^+ as stated above) can explain the benefit of this BK activator compound (Fig. 6) on the reduced PC12 neurite outgrowth and cell viability (Fig. 7) and on the mitochondrial content, also in PC12 cells (Fig. 8).

On the other hand, the presence of BK_{G354S} mutant channels both in the plasma membrane and the mitochondrial membrane

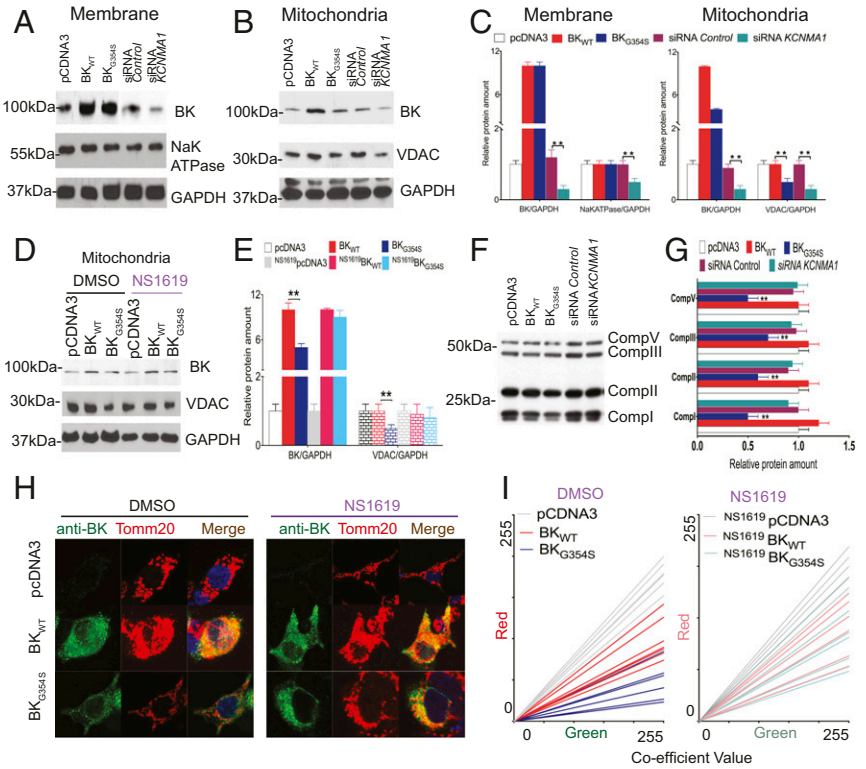

Fig. 8. The mutated BK_{G354S} channel induces a selective toxicity on mitochondria. (*A*) The protein level of BK_{WT} and BK_{G354S} in membrane fraction remains constant. (*B*) The protein level of BK_{G354S} in the mitochondrial fraction and the mitochondrial marker VDAC are decreased proportionally. (*C*) Quantitation of protein levels in *A* and *B* ($n \geq 6$; $^*P < 0.05$; $^{**}P < 0.01$; $^{***}P < 0.001$). (*D* and *E*) Representative blot (*D*) and quantitation (*E*) show NS1619 recovered the protein levels of BK channel and mitochondria. (*F* and *G*) OXPHOS proteins were decreased in cells expressing BK_{G354S} relative to BK_{WT}-expressing cells. (*H* and *I*) HEK cells overexpressing BK_{WT} or BK_{G354S} are stained with mitochondrial indicator Tomm20 in red; BK_{WT} and BK_{G354S} are stained with anti-BK antibody in green. Representative images show colocalization of BK and mitochondria with or without NS1619 treatment. The intensity of mitochondrial indicator Tommo20 is decreased in BK_{G354S}-expressing cells. NS1619 recovered the colocalization pattern between BK_{G354} channel and mitochondria (*I*).

would lead to the following: first, an increase in cytoplasmic Na^+ concentration during neuronal activity similar to that produced during ischemia (43); and second, as a consequence of the reduction or loss of mitoBK, the cytoprotective effect of the activation of mitoBK is lost (44). Therefore, NS1619 has the double beneficial role of inhibiting the mutant channels reducing the deleterious effect of the mutant channels present in the plasma and mitochondrial membrane and activating the remaining BK_{WT} channels partially recovering the cytoprotective effect of mitoBK channel.

The transient beneficial effect of chlorzoxazone, a mixed SK/BK channel activator, may be attributed to the activation of residual SK channels as well, which may have even been upregulated in the disease context.

Although the association of other LOF K^+ channel mutations in the ataxia (1, 3, 6) suggests that a persistent depolarized neuronal state is a common pathological pathway, determining the subcellular sites of action of the toxic effect of these mutations will provide significant insight into the pathogenesis of SCAs. BK channels are widely expressed throughout the central nervous system and are abundant in cerebellar Purkinje cells. Together with SK channels, they play a key role in quickly repolarizing the cell membrane when the intracellular Ca^{2+} concentration is increased, as well as in shaping the afterhyperpolarization potential, especially in mature Purkinje cells (45, 46). Both BK and SK channels are also present in membranes of organelles, for example in the inner mitochondrial membrane (47) and in the inner nuclear membrane (48, 49), where they have similar biophysical and pharmacological properties. In mitochondria, they play a role in calcium retention capacity coupled to the permeability transition pore.

Thus, in the mitochondrial context, the effects of BK_{G354S} are different. In the present study, BK_{G354S} confers a toxic effect in cultured cell lines and impairs neurite outgrowth in neuronal precursor cells. We also find that BK_{G354S} is associated with dysfunctional, disrupted, and depleted mitochondria. Knockdown of the BK channel gene using siRNA replicates these cellular abnormalities. The channel mitoBK, one splicing variant of BK_{WT}, is thought to protect the mitochondrial matrix from Ca^{2+} overload by depolarizing the inner membrane and therefore by decreasing its polarization voltage, the main driving force for Ca^{2+} entry (44, 50). The driving force for K^+ is the voltage across the inner membrane (approximately −160 mV negative in the matrix), since K^+ concentration in the cytoplasm and in the mitochondrial matrix are similar. In the case of BK_{G354S} being present in the inner membrane of mitochondria, coassembled or not with mitoBK, its decreased unitary conductance and its partial Na^+ permeability must be considered. The decreased unitary conductance would disrupt the protective effect of the channel against intracellular Ca^{2+} increases and mitochondrial Ca^{2+} buffering, a hypothesis corroborated by our findings in this present work and also by effects of experimentally blockade with paxillin, a specific BK blocker (51). As explained above, the fact that a known BK channel activator such as NS1619 blocks the BK_{G354S} mutant channel suggests that the improved survival of cells expressing the mutant may result from both actions of the drug, particularly on mitoBK, i.e., blocking the deleterious Na^+ conductance of the mutant channel as well as increasing the activity of BK_{WT} channels only (Fig. 6) (44).

At present, there are no selective BK activators approved for human use. However, based on these findings, we performed an

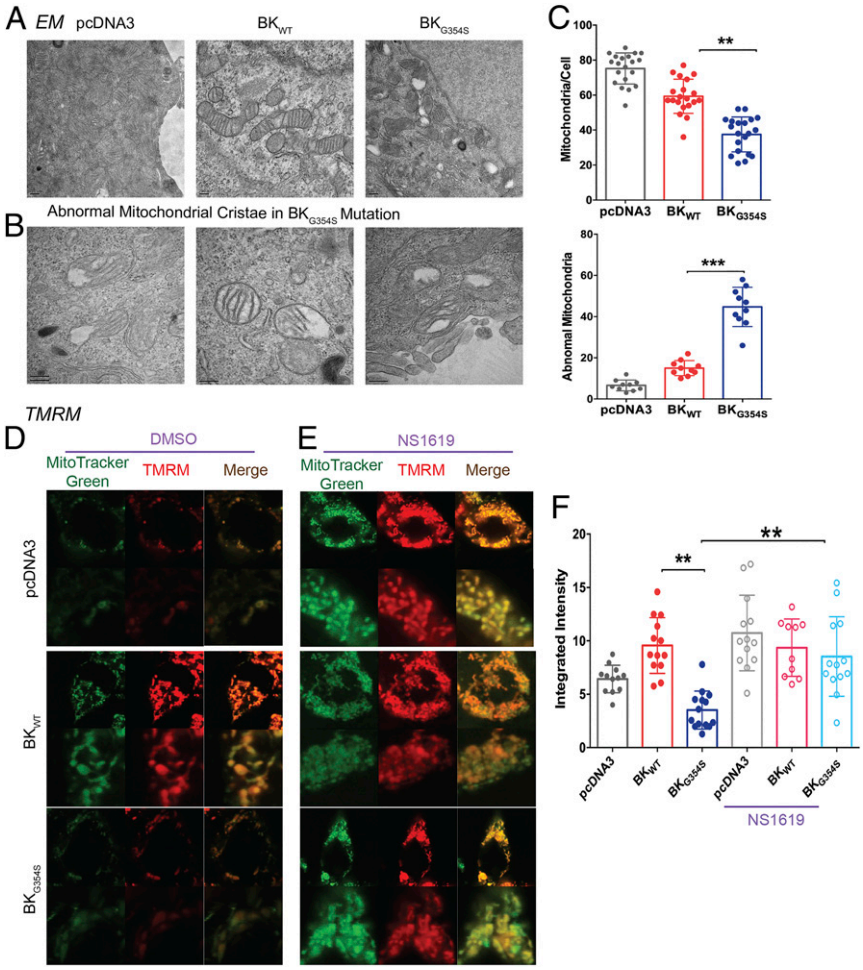

Fig. 9. Abnormal mitochondrial ultrastructure and decreased mitochondrial potential in HEK cells overexpressing BK_{G354S}, which can be rescued by NS1619. (*A*) Representative EM images show increased abnormal mitochondria in BK_{G354S} overexpression cell compared with a population of normal mitochondria in pcDNA3 and BK_{WT} overexpression cell. (*B*) Representative EM images show a diverse pattern of abnormal mitochondrial cristae in BK_{G354S} mutation. (*C*) Quantitation of number of mitochondria per cell and percentage of abnormal cristae ($n \geq 6$; $^*P < 0.05$; $^{**}P < 0.01$; $^{***}P < 0.001$). (*D* and *E*) HEK cells overexpressing BK_{WT} or BK_{G354S} are stained with MitoTracker green in green and TMRM in red. Representative images of TMRM decreased in BK_{G354S} overexpression cell compared with that in pcDNA3 and BK_{WT} overexpression cell (*D*); however, NS1619 treatment was able to recover TMRM expression in BK_{G354S} overexpression cell (*E*). (*F*) Quantitation of TMRM and MitoTracker integrated intensity in *D* and *E* ($n \geq 6$; $^{**}P < 0.01$).

empiric therapeutic challenge to explore the effect of a nonspecific BK/SK activator, chlorzoxazone, in the proband. The patient was evaluated by semiquantitative clinical and performance measures by blinded investigators, before and after the initiation of a standard therapeutic dose of this muscle relaxant. A statistically significant improvement was noted in the patient, although disease progression continued despite therapy. One explanation for these observations is that the improvement resulted from the effect on the plasma membrane SK and BK channels, while the disease progressed due to a lack of effect of the drug on the altered ion selectivity and on mitochondrial BK channels.

Mice with targeted deletion of BK channel α-subunit ($BK^{-/-}$) have predominantly a cerebellar phenotype with intention tremor, gait incoordination, and impaired eye-blink conditioning (a classic form of cerebellar motor learning). Surprisingly, these animals show no cerebellar degeneration. We found a similar picture in a mouse model induced by AAV delivery of the BK_{G354S} mutation. This is in contrast to two siblings with the more widespread motor system disorder and marked cerebellar atrophy, attributed to homozygous LOF mutations in the BK channel. We speculate that the difference relates to age differences, or the role of compensatory pathways. The present patient has a milder phenotype in which progressive ataxia began at age 8 y, attributed to a BK channel LOF mutation.

Studies of a mouse model for another form of ataxia, SCA1, provided a possible explanation that incorporates an integrated model. In SCA1 mice, induced by genetic overexpression of the ataxin-1 protein bearing an expanded polyglutamine repeat, secondary loss of BK channel expression is accompanied by reduced spontaneous discharges. The discharges reappear during Purkinje cell shrinkage. The authors were able to rescue the cells from shrinkage by pharmacologic activation or overexpression of normal BK channels. They suggest that the shrinkage is a homeostatic adaptation to restore Purkinje cell firing in the absence of BK channels (52). However, again the viability of the mitochondria has not been evaluated in any of these mouse ataxia models.

In summary, our studies identify another genetic cause of progressive ataxia. This LOF mutation in the selectivity filter of the BK channel supports the view that delayed neuronal repolarization due to impaired potassium channel function in the membrane in addition to reduced BK channel function in the mitochondria are potential mechanisms for Purkinje cell degeneration leading to cerebellar ataxia as well as developmental delay.

Materials and Methods

The materials and methods are described at length in *SI Appendix, SI Materials and Methods*. This includes human DNA samples, WES, cell culture, transient transfection, immunofluorescence staining, mitochondrial staining, cell death analysis, preparation of cell membranes and mitochondrial fractionation, antibody, retroviral transduction, live-cell imaging, expression in *Xenopus* oocytes, electrophysiology, injection of AAV9 into the ventricle of neonatal WT mice, moving platform posturography, and statistical analysis. Studies using human subjects were carried out with informed consent in accordance with the Institutional Review Board at the University of Chicago.

Data Availability. All DNA plasmids and bacterial strains used in this study are available at Dryad (https://doi.org/10.5061/dryad.1ns1rn8qk). All data generated and analyzed over the course of the current study are included within the manuscript or *SI Appendix*.

ACKNOWLEDGMENTS. This work was supported by NIH Grants R01NS082788, R01NS094665, and R21NS094872-01 (to C.M.G.), and R01GM030376 and R21-EY027101 (to F.B.); by University of Chicago Big Vision Grant (to C.M.G.); and by Fondecyt Grants 1150273 and 1190203, and the US Air Force Office of Scientific Research under Award A9550-16-1-0384 (to R.L.). This work was also supported by Centro Interdisciplinario de Neurociencia de Valparaiso, a Millennium Institute supported by the Millennium Scientific Initiative of the Chilean Ministry of Economy, Development, and Tourism (P029-022-F). We thank Yimei Chen at the University of Chicago Electron Microscopy Core Facility for the sample preparation and imaging service. We thank Dr. Vytas Bindokas at the University of Chicago Microscopy Core Facility for the imaging service.

1. D. L. Browne *et al.*, Episodic ataxia/myokymia syndrome is associated with point mutations in the human potassium channel gene, KCNA1. *Nat. Genet.* **8**, 136–140 (1994).
2. M. Coutelier *et al.*, A recurrent mutation in CACNA1G alters Cav3.1 T-type calcium-channel conduction and causes autosomal-dominant cerebellar ataxia. *Am. J. Hum. Genet.* **97**, 726–737 (2015).
3. M. C. D'Adamo, P. Imbrici, F. Sponcichetti, M. Pessia, Mutations in the KCNA1 gene associated with episodic ataxia type-1 syndrome impair heteromeric voltage-gated K^+ channel function. *FASEB J.* **13**, 1335–1345 (1999).
4. A. Duarri *et al.*, Mutations in potassium channel kcnd3 cause spinocerebellar ataxia type 19. *Ann. Neurol.* **72**, 870–880 (2012).
5. A. Duarri *et al.*, The L450F [corrected] mutation in KCND3 brings spinocerebellar ataxia and Brugada syndrome closer together. *Neurogenetics* **14**, 257–258 (2013).
6. K. P. Figueroa *et al.*, KCNC3: Phenotype, mutations, channel biophysics—a study of 260 familial ataxia patients. *Hum. Mutat.* **31**, 191–196 (2010).
7. K. P. Figueroa *et al.*, Frequency of KCNC3 DNA variants as causes of spinocerebellar ataxia 13 (SCA13). *PLoS One* **6**, e17811 (2011).
8. J. Jen, Calcium channelopathies in the central nervous system. *Curr. Opin. Neurobiol.* **9**, 274–280 (1999).
9. C. Marelli, C. Cazeneuve, A. Brice, G. Stevanin, A. Dürr, Autosomal dominant cerebellar ataxias. *Rev. Neurol. (Paris)* **167**, 385–400 (2011).
10. F. A. Nascimento, D. M. Andrade, Myoclonus epilepsy and ataxia due to potassium channel mutation (MEAK) is caused by heterozygous KCNC1 mutations. *Epileptic Disord.* **18**, 135–138 (2016).
11. K. Smets *et al.*, First de novo KCND3 mutation causes severe Kv4.3 channel dysfunction leading to early onset cerebellar ataxia, intellectual disability, oral apraxia and epilepsy. *BMC Med. Genet.* **16**, 51 (2015).
12. R. Latorre *et al.*, Molecular determinants of BK channel functional diversity and functioning. *Physiol. Rev.* **97**, 39–87 (2017).
13. C. S. Bailey, H. J. Moldenhauer, S. M. Park, S. Keros, A. L. Meredith, *KCNMA1*-linked channelopathy. *J. Gen. Physiol.* **151**, 1173–1189 (2019).
14. W. Du *et al.*, Calcium-sensitive potassium channelopathy in human epilepsy and paroxysmal movement disorder. *Nat. Genet.* **37**, 733–738 (2005).
15. M. Sausbier *et al.*, Cerebellar ataxia and Purkinje cell dysfunction caused by Ca^{2+}-activated K^+ channel deficiency. *Proc. Natl. Acad. Sci. U.S.A.* **101**, 9474–9478 (2004).
16. L. Liang *et al.*, De novo loss-of-function KCNMA1 variants are associated with a new multiple malformation syndrome and a broad spectrum of developmental and neurological phenotypes. *Hum. Mol. Genet.* **28**, 2937–2951 (2019).
17. B. Tabarki, N. AlMajhad, A. AlHashem, R. Shaheen, F. S. Alkuraya, Homozygous KCNMA1 mutation as a cause of cerebellar atrophy, developmental delay and seizures. *Hum. Genet.* **135**, 1295–1298 (2016).
18. Z. B. Zhang, M. Q. Tian, K. Gao, Y. W. Jiang, Y. Wu, De novo KCNMA1 mutations in children with early-onset paroxysmal dyskinesia and developmental delay. *Mov. Disord.* **30**, 1290–1292 (2015).
19. G. Yeşil *et al.*, Expanding the phenotype of homozygous *KCNMA1* mutations; dyskinesia, epilepsy, intellectual disability, cerebellar and corticospinal tract atrophy. *Balkan Med. J.* **35**, 336–339 (2018).
20. G. Edwards, A. Niederste-Hollenberg, J. Schneider, T. Noack, A. H. Weston, Ion channel modulation by NS 1619, the putative BKCa channel opener, in vascular smooth muscle. *Br. J. Pharmacol.* **113**, 1538–1547 (1994).
21. M. Holland, P. D. Langton, N. B. Standen, J. P. Boyle, Effects of the BKCa channel activator, NS1619, on rat cerebral artery smooth muscle. *Br. J. Pharmacol.* **117**, 119–129 (1996).
22. S. P. Olesen, E. Munch, P. Moldt, J. Drejer, Selective activation of Ca^{2+}-dependent K^+ channels by novel benzimidazolone. *Eur. J. Pharmacol.* **251**, 53–59 (1994).
23. Y.-C. Liu, Y.-K. Lo, S.-N. Wu, Stimulatory effects of chlorzoxazone, a centrally acting muscle relaxant, on large conductance calcium-activated potassium channels in pituitary GH_3 cells. *Brain Res.* **959**, 86–97 (2003).
24. X. Li *et al.*, De novo BK channel variant causes epilepsy by affecting voltage gating but not Ca^{2+} sensitivity. *Eur. J. Hum. Genet.* **26**, 220–229 (2018).
25. I. Adzhubei, D. M. Jordan, S. R. Sunyaev, Predicting functional effect of human missense mutations using PolyPhen-2. *Curr. Protoc. Hum. Genet.* 76, 7.20.1–7.20.41 (2013).
26. P. C. Ng, S. Henikoff, SIFT: Predicting amino acid changes that affect protein function. *Nucleic Acids Res.* **31**, 3812–3814 (2003).
27. N. Makhseed *et al.*, Carnitine transporter defect due to a novel mutation in the SLC22A5 gene presenting with peripheral neuropathy. *J. Inherit. Metab. Dis.* **27**, 778–780 (2004).
28. S. Srivastava *et al.*, BRAT1 mutations present with a spectrum of clinical severity. *Am. J. Med. Genet. A.* **170**, 2265–2273 (2016).
29. M. Zatz, F. de Paula, A. Starling, M. Vainzof, The 10 autosomal recessive limb-girdle muscular dystrophies. *Neuromuscul. Disord.* **13**, 532–544 (2003).
30. X. Tao, R. K. Hite, R. MacKinnon, Cryo-EM structure of the open high-conductance Ca^{2+}-activated K^+ channel. *Nature* **541**, 46–51 (2017).
31. L. Heginbotham, Z. Lu, T. Abramson, R. MacKinnon, Mutations in the K^+ channel signature sequence. *Biophys. J.* **66**, 1061–1067 (1994).
32. G. Gessner *et al.*, Molecular mechanism of pharmacological activation of BK channels. *Proc. Natl. Acad. Sci. U.S.A.* **109**, 3552–3557 (2012).
33. Y. Miyazaki, X. Du, S. Muramatsu, C. M. Gomez, An miRNA-mediated therapy for SCA6 blocks IRES-driven translation of the CACNA1A second cistron. *Sci. Transl. Med.* **8**, 347ra94 (2016).
34. X. Du *et al.*, Second cistron in CACNA1A gene encodes a transcription factor mediating cerebellar development and SCA6. *Cell* **154**, 118–133 (2013).
35. S. Romano *et al.*, Riluzole in patients with hereditary cerebellar ataxia: A randomised, double-blind, placebo-controlled trial. *Lancet Neurol.* **14**, 985–991 (2015).
36. G. Ristori *et al.*, Riluzole in cerebellar ataxia: A randomized, double-blind, placebo-controlled pilot trial. *Neurology* **74**, 839–845 (2010).
37. T. Schmitz-Hübsch *et al.*, Scale for the assessment and rating of ataxia: Development of a new clinical scale. *Neurology* **66**, 1717–1720 (2006).
38. P. Imbrici, M. C. D'Adamo, A. Cusimano, M. Pessia, Episodic ataxia type 1 mutation F184C alters Zn^{2+}-induced modulation of the human K^+ channel Kv1.4-Kv1.1/Kvbeta1.1. *Am. J. Physiol. Cell Physiol.* **292**, C778–C787 (2007).
39. M. A. Corbett *et al.*, Dominant KCNA2 mutation causes episodic ataxia and pharmacoresponsive epilepsy. *Neurology* **87**, 1975–1984 (2016).
40. P. Zerr, J. P. Adelman, J. Maylie, Characterization of three episodic ataxia mutations in the human Kv1.1 potassium channel. *FEBS Lett.* **431**, 461–464 (1998).
41. R. A. Ophoff *et al.*, Familial hemiplegic migraine and episodic ataxia type-2 are caused by mutations in the Ca^{2+} channel gene CACNL1A4. *Cell* **87**, 543–552 (1996).
42. T. Irie, Y. Matsuzaki, Y. Sekino, H. Hirai, Kv3.3 channels harbouring a mutation of spinocerebellar ataxia type 13 alter excitability and induce cell death in cultured cerebellar Purkinje cells. *J. Physiol.* **592**, 229–247 (2014).
43. M. Murata, M. Akao, B. O'Rourke, E. Marbán, Mitochondrial ATP-sensitive potassium channels attenuate matrix Ca^{2+} overload during simulated ischemia and reperfusion: Possible mechanism of cardioprotection. *Circ. Res.* **89**, 891–898 (2001).
44. T. Sato, T. Saito, N. Saegusa, H. Nakaya, Mitochondrial Ca^{2+}-activated K^+ channels in cardiac myocytes: A mechanism of the cardioprotective effect and modulation by protein kinase A. *Circulation* **111**, 198–203 (2005).
45. M. D. Womack, K. Khodakhah, Characterization of large conductance Ca^{2+}-activated K^+ channels in cerebellar Purkinje neurons. *Eur. J. Neurosci.* **16**, 1214–1222 (2002).
46. M. D. Womack, C. Hoang, K. Khodakhah, Large conductance calcium-activated potassium channels affect both spontaneous firing and intracellular calcium concentration in cerebellar Purkinje neurons. *Neuroscience* **162**, 989–1000 (2009).
47. H. Singh *et al.*, $MitoBK_{Ca}$ is encoded by the *Kcnma1* gene, and a splicing sequence defines its mitochondrial location. *Proc. Natl. Acad. Sci. U.S.A.* **110**, 10836–10841 (2013).
48. H. Singh, E. Stefani, L. Toro, Intracellular BK_{Ca} (iBK_{Ca}) channels. *J. Physiol.* **590**, 5937–5947 (2012).
49. B. Li, T. M. Gao, Functional role of mitochondrial and nuclear BK channels. *Int. Rev. Neurobiol.* **128**, 163–191 (2016).
50. C. E. Gavin, K. K. Gunter, T. E. Gunter, Manganese and calcium efflux kinetics in brain mitochondria. Relevance to manganese toxicity. *Biochem. J.* **266**, 329–334 (1990).
51. W. Xu *et al.*, Cytoprotective role of Ca^{2+}-activated K^+ channels in the cardiac inner mitochondrial membrane. *Science* **298**, 1029–1033 (2002).
52. J. M. Dell'Orco *et al.*, Neuronal atrophy early in degenerative ataxia is a compensatory mechanism to regulate membrane excitability. *J. Neurosci.* **35**, 11292–11307 (2015).
53. F. Bezanilla, C. M. Armstrong, Inactivation of the sodium channel. I. Sodium current experiments. *J. Gen. Physiol.* **70**, 549–566 (1977).